

A yeast splicing factor is localized in discrete subnuclear domains

David J.Elliott, Douglas S.Bowman¹,
Nadja Abovich, Fredric S.Fay¹ and
Michael Rosbash

Howard Hughes Medical Institute and Department of Biology,
Brandeis University, Waltham, MA 02254, USA, and ¹Biomedical
Imaging Group, Program in Molecular Medicine, University of
Massachusetts Medical School, 373 Plantation Street, Worcester,
MA 01605, USA

Communicated by I.Mattaj

Digital imaging microscopy has been used to visualize the splicing protein PRP6p and three other yeast nuclear proteins. The results show that PRP6p is uniquely localized to discrete subnuclear regions. A combination of cytological and biochemical assays suggests that these sites can be saturated when the protein is overexpressed and likely correspond to the location of U4/U6 snRNPs. The observations indicate that some splicing components are located in discrete subregions of the yeast nucleus, similar to the situation described for the mammalian nucleus.

Key words: digital imaging microscopy/nuclear organization/pre-mRNA splicing/yeast

Introduction

Most eukaryotic genes contain introns, which are removed from pre-mRNA in large ribonucleoprotein complexes called spliceosomes (Brody and Abelson, 1985; Friendewey and Keller, 1985; Grabowski *et al.*, 1985). *In vitro* spliceosome formation requires the sequential binding of factors (both protein and snRNP) to conserved intron sequences (Grabowski and Sharp, 1986; Pikielny *et al.*, 1986; Konarska and Sharp, 1987; Bindereif and Green, 1987; Lamond *et al.*, 1988; Séraphin and Rosbash, 1989; Lamm *et al.*, 1991; Séraphin *et al.*, 1991). Although splicing has been extensively characterized using soluble whole cell or nuclear extracts, it is not yet known how this process is spatially organized in the nucleus, nor how it is functionally integrated with transcription and mRNA export to the cytoplasm. Whereas soluble factors are simultaneously available for *in vitro* spliceosome formation, factors may be compartmentalized *in vivo* and only available at certain times and in certain locations. Indeed, immunofluorescence experiments have shown that mammalian splicing factors occupy distinct locations (Fu and Maniatis, 1990; Carmo-Fonseca *et al.*, 1991, 1992; Carter *et al.*, 1991; Gall, 1991; Spector *et al.*, 1991; Huang and Spector, 1992), but it is difficult to assign specific functions to these subnuclear regions.

Biochemical experiments have shown that splicing and spliceosome assembly are similar if not identical in yeast (*Saccharomyces cerevisiae*) and higher eukaryotes (Guthrie,

1991; Rosbash and Séraphin, 1991; Green, 1991; Ruby and Abelson, 1991), making yeast an important organism for *in vitro* studies. Also, the genetic and molecular tools available in the yeast system have led to the identification of a large number of gene products that participate in spliceosome assembly and splicing (PRP proteins) (Rosbash *et al.*, 1981; Vijayraghavan *et al.*, 1989; Ruby and Abelson, 1991). However, the small size of the yeast nucleus, and perhaps its low snRNP content, have been a major obstacle to the analysis of the spatial organization of these factors.

We have examined the localization of nuclear components in yeast using digital imaging microscopy, which has enabled us to obtain high resolution images from low intensity signals. The results indicate that the splicing protein PRP6p is compartmentalized within the yeast nucleus by binding to a finite number of localized receptors. The evidence suggests that these receptors are the U4/U6 snRNPs themselves. In addition, we show for the first time that RNA polymerase II is spatially restricted to its presumed site of action (the nucleoplasm), as a result of exclusion from the nucleolus. The appropriate localization of factors within the nucleus may be an important factor contributing to proper gene expression.

Results

Visualization of RNA polymerase II

Digital imaging microscopy has been previously used to localize a yeast $\alpha 2$ repressor–*LacZ* fusion protein to the nucleus and to the nuclear envelope (Hall *et al.*, 1990). To demonstrate that we could resolve detail within the yeast nucleus, we initially examined the distribution of a subunit of RNA polymerase II. Detection was achieved with a monoclonal antibody (12CA5) which recognizes a nine amino acid epitope from flu virus, the sequence for which was inserted into the reading frame of an RNA polymerase II subunit (Kolodziej *et al.*, 1990). Cells were prepared for immunofluorescence (Davis and Fink, 1990) and then visualized using digital imaging microscopy (Agard *et al.*, 1989; Fay *et al.*, 1989). A series of optical sections (0.125 μm apart) were taken through a yeast nucleus and processed to reverse the distortion introduced by the optics.

The tagged RNA polymerase II strain showed a relatively homogeneous staining pattern (Figure 1), whereas strains lacking the flu epitope gave no detectable nuclear immunofluorescence (data not shown). Although RNA polymerase II is likely to be in excess of cellular requirements in yeast (R.Young, personal communication), regions of somewhat more intense fluorescence (Figure 1) might correspond to sites of more active transcription similar to those described in mammalian cells (Fakan and Puvion, 1980; Spector, 1990). The cells were also stained with RL1, a monoclonal antibody which recognizes nuclear pores (and hence defines the periphery of the nucleus). The pictures

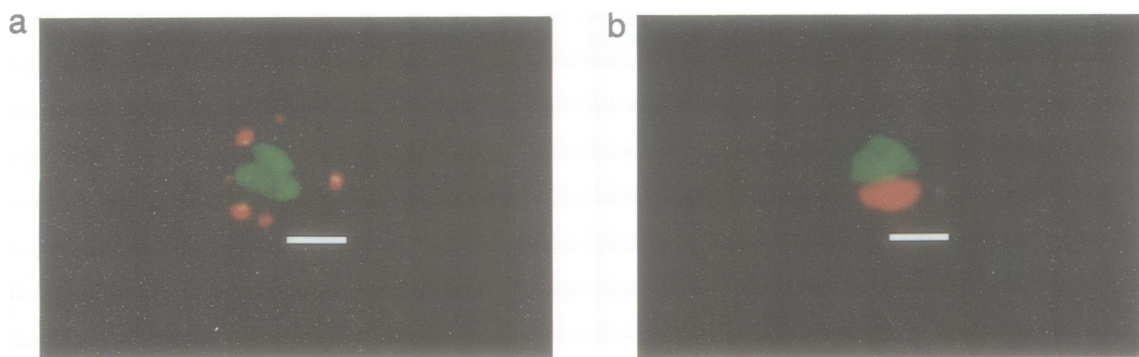


Fig. 1. Subnuclear localization of RNA polymerase II. (a) Double labelling of RNA polymerase II (green) and nuclear pores (red). RNA polymerase was visualized using McAb 12CA5 (a gift of I.Wilson) at a dilution of 1:100, and an FITC-conjugated goat anti-mouse IgG Fc-specific secondary antibody (Cappel). The nuclear pores were visualized using McAb RL1 (a gift of L.Gerace) at a dilution of 1:200, and a TRITC-conjugated goat anti-mouse IgM-specific secondary antibody (Cappel). (b) Double labelling of RNA polymerase II (green) and the nucleolus (red). RNA polymerase II was visualized using a McAb 12CA5 primary, and an FITC-conjugated sheep anti-mouse IgG (no cross-reaction to human) secondary antibody (Cappel). The nucleolus was visualized using autoimmune serum 1875 (a gift of S.Baserga and J.Steitz) and a Texas red-conjugated affinity purified goat anti-human IgG (minimum cross-reaction to mouse; Jackson Labs). Images obtained using different fluorochromes were superimposed by using a fluorescent bead visible at both wavelengths. The regions where these signals overlap appear white in the two colour images. Single optical sections are shown and, in the case of superimposed images, the sections are from equivalent points in the series. The calibration bar indicates 1 μ m.

indicated that RNA polymerase II was spatially restricted to a subregion of the nucleus (Figure 1a). RL1 immunostaining was heterogeneous; both punctate and larger, more irregular structures were detected which might correspond to nuclear pores or groups of nuclear pores (Maul, 1977; Hurt, 1988). The number of discrete structures stained by RL1 is consistent with the number of pores seen in electron microscope sections, which are of a comparable thickness (Nehrbass *et al.*, 1990). Double labelling with a nucleolar-specific antibody, 1875, showed that the spatial restriction of RNA polymerase II resulted from nucleolar exclusion (Figure 1b). In both cases (Figures 1a and b), a very small overlap in staining was apparent. This overlap may be real or may reflect a limit to the resolution of these microscopic procedures. We conclude that this procedure gives expected subnuclear distributions for a nuclear pore antigen, a nucleolar antigen and RNA polymerase II, including localization of RNA polymerase II within the nucleus.

Visualization of the splicing protein PRP6p

We next examined the distribution of a tagged version of the yeast splicing protein PRP6p. Mutations in this protein prevent U4/U6 snRNP addition *in vitro* and lead to pre-mRNA transport to the cytoplasm *in vivo* (Legrain and Rosbash, 1989; Abovich *et al.*, 1990). The same flu epitope had been used to tag an otherwise wild-type copy of PRP6p that is expressed from a centromeric plasmid in a strain containing a temperature-sensitive allele of the chromosomal *prp6* gene (strain PRP6YCP). This strain grows normally at the non-permissive temperature (37°C), indicating that the tagged *PRP6* gene rescues the temperature-sensitive growth of the mutant host strain (Abovich *et al.*, 1990). The 12CA5 monoclonal antibody immunoprecipitates U4/U6 snRNPs from this strain (Abovich *et al.*, 1990). F.Galisson and P.Legrain (manuscript in preparation) have independently observed that a polyclonal antibody directed against PRP6p immunoprecipitates U4/U6 snRNPs from wild-type strains.

Western blotting with a polyclonal anti-PRP6 antiserum showed that the endogenous mutant protein was undetectable at 37°C (also observed by F.Galisson and P.Legrain,

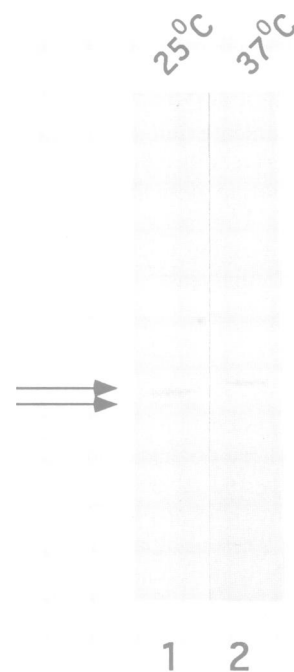


Fig. 2. Western blot of PRP6p. Protein from equivalent amounts of yeast splicing extract from strain PRP6YCP were separated on a 7.5% polyacrylamide-SDS gel. The splicing extracts were prepared from cells grown at 25°C and 37°C in lanes 1 and 2, respectively. The top arrow points to the tagged protein and the bottom arrow to the endogenous protein. Proteins were transferred to a nitrocellulose filter, which was probed with α -PRP6p IgG fraction a-FG62Ai8 (a kind gift of F.Galisson and P.Legrain) at a dilution of 1:5000.

personal communication), whereas at 25°C the tagged protein was detectable at somewhat higher levels than the temperature-sensitive protein (Figure 2). At 25°C, the level of the tagged protein was similar to that of the wild-type PRP6p from another strain that carried the chromosomal wild-type *PRP6* gene (data not shown). All of these observations indicate that the tagged PRP6p is biologically active, that it is a U4/U6 snRNP protein like wild-type PRP6p, and that it is present at a level comparable with that of PRP6p.

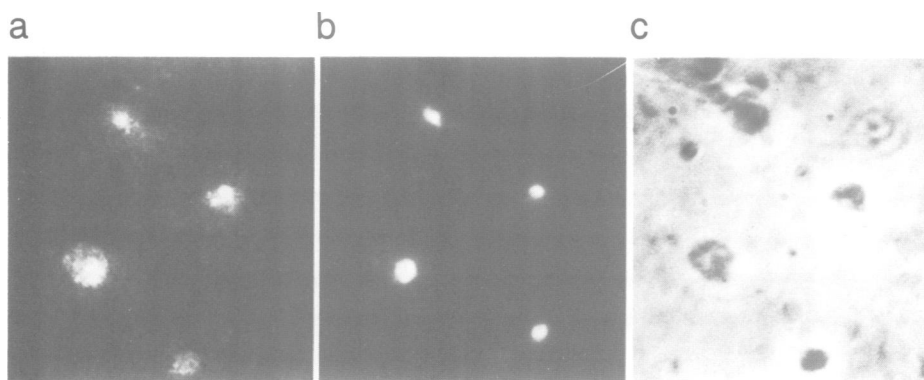


Fig. 3. Unprocessed image of the nuclear localization of PRP6p. (a) Localization of tagged PRP6p within yeast cells. The flu epitope was visualized as in Figure 1(a). (b) Localization of DNA within the same field of view using DAPI. (c) Phase contrast image. In each case a single image of the cells was taken and not processed to remove out-of-focus light, unlike the pictures in Figures 1 and 4.

When visualized by indirect immunofluorescence using the anti-tag monoclonal primary antibody, prominent staining was observed within or near nuclei (Figure 3). Also apparent was a low level of cytoplasmic staining. This is due to non-specific background staining (data not shown), and a small fraction of the tagged PRP6p may even be cytoplasmic. The nuclear staining appeared granular. This is most clear in the lower left hand cell in Figure 3(a), where the image is taken through an equatorial plane of the nucleus. These images are unprocessed and also at a low magnification, which makes it more difficult to resolve subnuclear detail than in Figures 1 and 4.

When processed for microscopy by exactly the same procedures used above for the tagged RNA polymerase II strain, the tagged PRP6p reproducibly localized to multiple discrete sites both in the nuclei of intact cells (Figure 4a) and in isolated nuclei (Figure 4b). Within individual nuclei there were both strong and weak sites, independent of the plane of focus. The number of sites was estimated by counting through serial optical sections. In intact cells, the majority of nuclei were stained and there were $9.63 (\pm 2.2)$ sites/nucleus. A much smaller proportion of isolated nuclei were stained, and there were $6.8 (\pm 1.5)$ sites/nucleus. Double labelling with an anti-nucleolar antibody showed that this punctate staining was also predominantly nucleoplasmic, both in intact cells (Figure 4c) and in isolated nuclei (Figure 4d). In some cases, an overlap in signal was observed (e.g. Figure 4d). As described above for RNA polymerase II, this might be real or might reflect a limit to the light microscopic resolution.

When the tagged PRP6p was overexpressed from a high copy number plasmid (strain PRP6YEP), much higher levels were detected by Western blotting of total yeast protein (Figure 5, note dilutions). Immunofluorescence intensity was also much increased compared with strain PRP6YCP, but the staining was still restricted to the nucleus (Figures 4e and f, and data not shown). Since PRP6p overexpression does not affect the levels of other snRNP components (including U4/U6 snRNAs, data not shown), it is likely that PRP6p has a distinct nuclear localization signal and is not imported 'piggyback' as a component of an snRNP complex.

Although there were still visible nuclear subregions of more intense fluorescence in strain PRP6YEP, the pattern was much more uniform than that of PRP6YCP. Only the center of the nucleolus failed to stain with the anti-tag

antibody (Figure 4f). The dramatic decrease in the discrete punctate staining pattern indicates that the excess PRP6p had saturated its binding sites, suggesting that PRP6p is normally targeted or maintained at its punctate locations by binding to a finite number of specific receptors.

Association of PRP6p with snRNPs

Experiments were carried out to determine the extent to which the tagged PRP6p was associated with U4/U6 snRNPs. After ultracentrifugation of splicing extracts at 300 mM KCl, a substantial fraction of the splicing snRNPs are in the pellet (Abovich *et al.*, 1990; Séraphin *et al.*, 1991) and this is also true for tagged PRP6p (Figure 5, lanes 4–6). The distribution of tagged PRP6p between pellet and supernatant fractions is similar to that of U4 snRNA (Séraphin *et al.*, 1991), suggesting that much of the tagged PRP6p is associated with U4/U6 snRNP. In contrast, only a subset of the U4/U6 population (e.g. U4/U5/U6 snRNPs) may be associated with PRP6p, because the immunoprecipitation of U4/U6 snRNP with the anti-tag antibody is relatively inefficient (data not shown).

In similar experiments with extracts from the PRP6YEP strain, there was more tagged protein and a greater proportion was in the supernatant fraction, suggesting that the extra PRP6p was not snRNP-associated (Figure 5, lanes 1–3). Consistent with this suggestion, only marginally more U4/U6/U5 snRNPs were immunoprecipitated with 12CA5 antibodies from PRP6YEP-derived extracts than from PRP6YCP-derived extracts (Figure 6). Taken together with previous results (Abovich *et al.*, 1990; Séraphin *et al.*, 1991), the data suggest that only in the PRP6YCP strain is much and perhaps all of the tagged PRP6p in U4/U6 snRNPs. Although we cannot exclude the possibility that the immunofluorescence microscopy is only visualizing a small fraction of PRP6p that is not snRNP associated, we infer that the punctate staining regions are the cytological locations of U4/U6 snRNPs or a fraction thereof.

Discussion

The results reported here show that PRP6p, and by inference U4/U6 snRNPs, is located in discrete subnuclear domains in yeast. This result is in contrast with two previous immunoelectron microscope studies that localized splicing factors within the yeast nucleus. One indicated that trimethyl

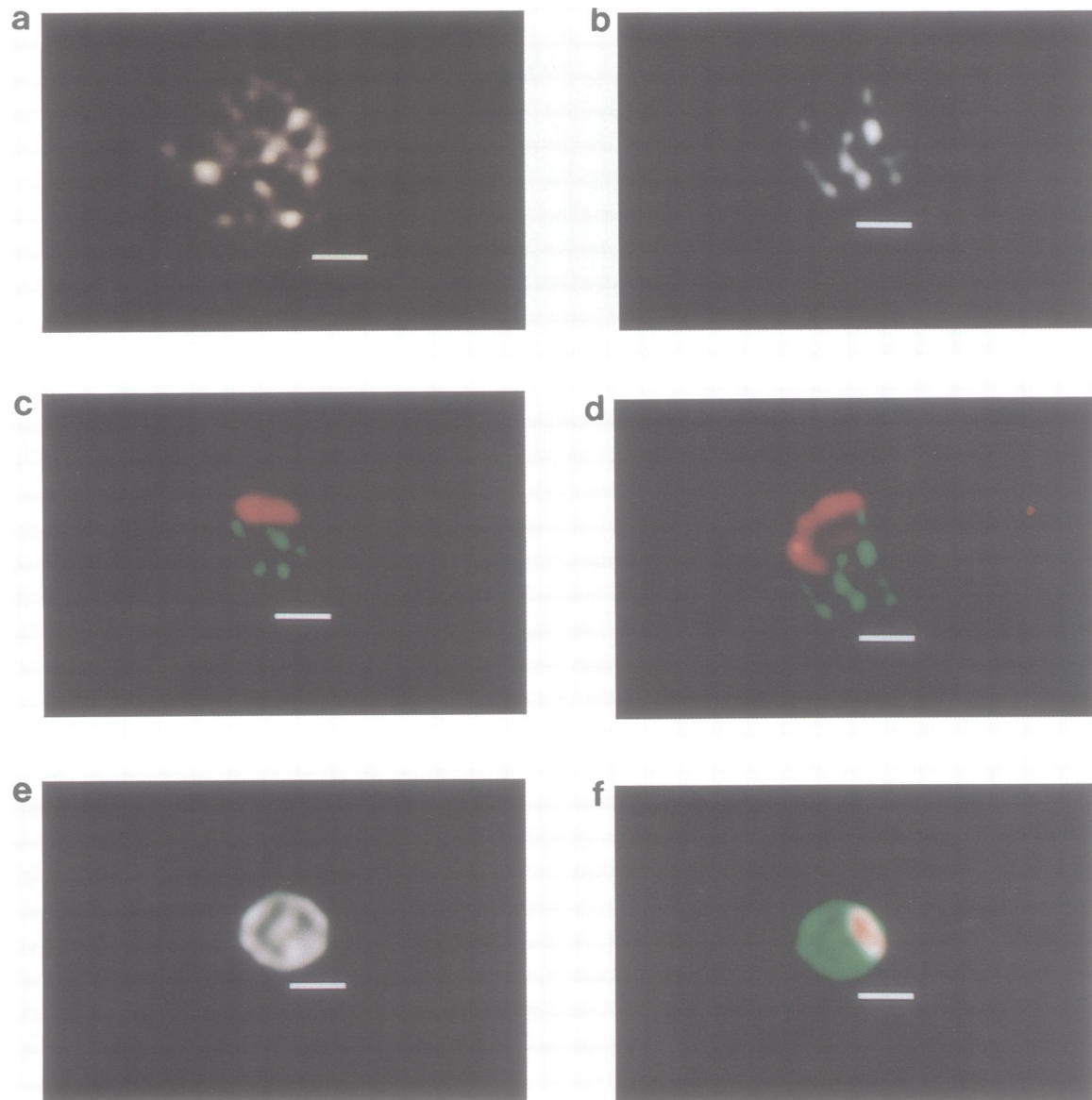


Fig. 4. Subnuclear localization of tagged PRP6p. (a) Distribution of tagged PRP6p in intact PRP6YCP cells. PRP6p was visualized as in Figure 1(a). (b) Distribution of tagged PRP6p in nuclei isolated from strain PRP6YCP. PRP6p was visualized as in Figure 1(a), and no signal was observed in nuclei isolated from cells which did not contain tagged PRP6p (not shown). (c) Double labelling of tagged PRP6p (green) and the nucleolus (red) in intact PRP6YCP cells. Immunofluorescence procedures were carried out as for Figure 1. (d) Double labelling of tagged PRP6p (green) and the nucleolus (red) in nuclei isolated from PRP6YCP cells. Immunofluorescence procedures were carried out as for Figure 1, and this is the same cell shown in Figure 3(b). (e) Distribution of tagged PRP6p in PRP6YEP cells. PRP6p was visualized as in Figure 1(a). (f) Double labelling of tagged PRP6p and the nucleolus in a PRP6YEP cell. Immunofluorescence and microscopic procedures were carried out as for Figure 1(b), and this is the same cell shown in Figure 3(e). The data are presented as described in the legend for Figure 1.

cap structures were predominantly nucleolar and suggested that the yeast splicing machinery might be spatially organized in a manner different from that in higher eukaryotes (Potashkin *et al.*, 1990). The other indicated that the yeast splicing factor PRP11p was predominantly perinuclear (Chang *et al.*, 1988), a location also different from what is typically observed in mammalian cells. However, as in mammalian cells, different yeast splicing proteins may have different subnuclear locations (Zamore and Green, 1991).

In the case of mammalian splicing factors, two overlapping distributions have been identified. Antibodies to many splicing components (e.g. Sm, Sc35, m₃G cap) stain a large number of punctate nuclear subregions called 'speckles'. The second distribution is a small number of 'foci', which

correspond to structures previously identified as coiled bodies (Fu and Maniatis, 1990; Carmo-Fonseca *et al.*, 1991, 1992; Carter *et al.*, 1991; Gall, 1991; Spector *et al.*, 1991; Wang *et al.*, 1991; Huang and Spector, 1992). It is not clear which of these two patterns (if any) corresponds to the locations of active splicing, nor which of these two patterns corresponds more closely to that of the yeast PRP6p.

Whereas the function of the yeast punctate staining regions is also unknown, depletion experiments suggest that the snRNP population is in substantial excess over what is required to support normal growth and splicing (Siliciano *et al.*, 1987; Séraphin and Rosbash, 1989; Séraphin *et al.*, 1991). Although we cannot exclude the possibility that another step is more limiting for splicing and growth, this

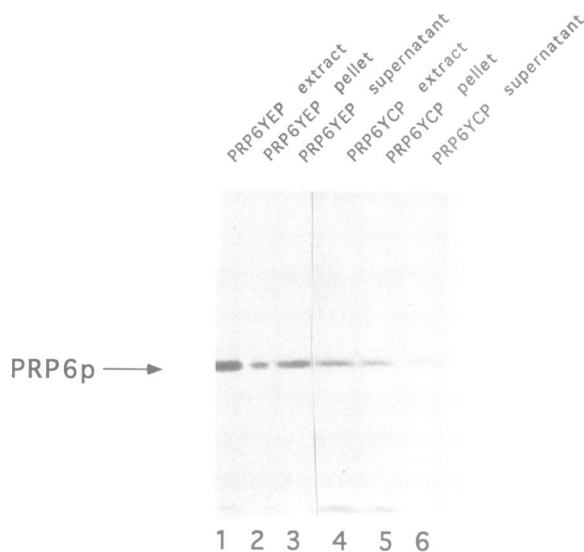


Fig. 5. Western blot of tagged PRP6p protein in fractionated extracts. Yeast extracts from strains PRP6YCP and PRP6YEP were fractionated into pellets and supernatants as described (Abovich *et al.*, 1990; Séraphin *et al.*, 1991). For each strain the protein from equivalent amounts of extract was separated on a 7.5% polyacrylamide-SDS gel, blotted and probed with McAb 12CA5 at a dilution of 1:1000. Lanes 1, 2 and 3 contain protein from strain PRP6YEP, and lanes 4, 5 and 6 from strain PRP6YCP. Lanes 1, 2 and 3 were loaded with 1/4 as much protein as lanes 4, 5 and 6, respectively.

observation suggests that much of the visualized PRP6p-U4/U6 snRNP may not be engaged in active splicing. Future work will attempt to define further the function of the yeast subnuclear domains by examining the localization of PRP6p and other splicing proteins in mutants that are defective in specific steps of RNA maturation.

PRP6p might be directly anchored to some nuclear substructure such as the nuclear matrix (Jackson, 1991). In support of a direct association, PRP6p contains a TPR motif (Legrain and Choulika, 1990; Legrain *et al.*, 1991), which has been shown to occur in a number of other yeast nuclear proteins, including one demonstrated to be a nuclear matrix protein (*nuc2⁺*) (Hirano *et al.*, 1990). PRP6p also has three stretches of basic amino acids at its N-terminus (Legrain and Choulika, 1990). In higher eukaryotes, stretches of basic amino acids, predominantly arginine and serine, have been implicated in targeting splicing proteins to 'speckled' locations (Li and Bingham, 1991).

Alternatively, PRP6p might be indirectly anchored by virtue of its presence in the U4/U6 snRNP and might have no direct association with the nuclear substructure. The finite, specific PRP6p receptors referred to above would then be the U4/U6 snRNPs themselves, and any feature of these snRNPs might then be responsible for anchoring them to the nuclear subdomains. Consistent with this notion, the putative uncomplexed (i.e. non-snRNP) PRP6p in strain PRP6YEP localizes more poorly to the punctate regions (Figure 4e and f). These considerations suggest that the Ser-Arg domain present on many higher eukaryotic splicing factors might also facilitate subnuclear targeting indirectly, by promoting protein-protein (or protein-snRNP) associations (e.g. Zamore *et al.*, 1992) that are necessary

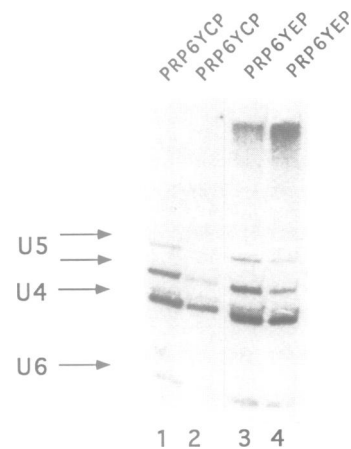


Fig. 6. Immunoprecipitation of snRNPs associated with tagged PRP6p. The equivalent of 10 μ l of extract from strains PRP6YCP and PRP6YEP was immunoprecipitated with 12CA5 antibody at a salt concentration of 300 mM KCl as previously described (Abovich *et al.*, 1990). The supernatants were reprecipitated with a fresh aliquot of 12CA5 antibody. Pellets were treated with proteinase K and phenol extracted. RNAs were separated on 4% polyacrylamide-7 M urea gels, which were electroblotted and hybridized with labelled snRNA probes. Lanes 1 and 2 show precipitated RNAs from strain PRP6YCP, and lanes 3 and 4 show RNAs from strain PRP6YEP. The two-step immunoprecipitation demonstrates that the first precipitation was relatively efficient (lane 1 > lane 2; lane 3 > lane 4), indicating that a comparison between lanes 1 and 3 is valid.

for the localization of the Ser-Arg-containing protein to the 'speckles'.

The results reported here indicate that the yeast splicing machinery may have a similar spatial organization to that of higher eukaryotes. This is surprising since the majority of yeast genes do not contain introns, and there is a comparative lack of complexity in yeast splicing processes; there are no known examples in yeast of regulated alternative splicing, a circumstance that might require sophisticated transcript management. The evolutionary conservation of nuclear organization between yeast and mammalian cells therefore suggests that it may be of fundamental importance to basic features of gene expression.

Materials and methods

Yeast strains

RNA polymerase II was visualized in yeast strain Z277, which expresses an epitope-tagged RPB3 (pol II) protein (Kolodziej *et al.*, 1990). Tagged PRP6p was detected in strains PRP6YCP and PRP6YEP. Strain PRP6YCP has previously been described as strain PRP6-5'-3'-HA (Abovich *et al.*, 1990). Strain PRP6YEP was identical, apart from carrying the epitope-tagged *PRP6* gene in the multicopy plasmid YEP24.

Indirect immunofluorescence

Cells were prepared for immunofluorescence according to the procedure of Davis and Fink (1990) except in the case of Figure 3 where the methanol fixation step was omitted. We found this improved the PRP6p staining while not affecting the overall staining pattern. Cells were visualized using digital imaging microscopy as described below. Primary and secondary antibodies were as indicated in the figure legends.

Isolation and staining of yeast nuclei

Nuclei were prepared according to the method of Hurt *et al.* (1988) up to the sucrose step gradient and then settled on polylysine-coated slides. Subsequent steps in the immunofluorescence protocol were then carried out as for intact cells.

Digital imaging microscopy

Digital images of the fluorescence distribution in single cells or nuclei were obtained using a Nikon 60× Planapo (NA = 1.4) objective on a Zeiss IM-35 microscope equipped for epifluorescence, as described previously (Fay et al., 1989). Briefly, images at various planes were obtained with a computer controlled focus mechanism and a Photometrics model 220 thermoelectrically cooled CCD. The duration of exposure of the specimen to the excitation source was controlled by a computer controlled shutter and wavelength selector system (MVI, Avon, MA). Camera and microscope functions were controlled and coordinated by a microcomputer and data acquired from the CCD were transferred to a Silicon Graphics workstation for further processing. Images were corrected for the camera dark current and for non-uniformities in sensitivity of the CCD detector; variations in light source intensity during a thorough focal series were corrected from measurements of the total light from the specimen at each plane, which for these small changes in focus reflect effectively only variations in light source intensity. The calibration of the microscope blurring was determined by measuring the instrument's point spread function as a series of optical sections at 0.125 μm intervals of a 0.19 μm diameter fluorescently labelled latex bead (Molecular Probes). The image restoration algorithm (Carrington et al., 1990; K.C.Carter, D.Bowman, W.Carrington, K.Fogarty, J.A.McNeil, F.S.Fay and J.Bentley Lawrence, submitted) used is based upon the theory of ill-posed problems and obtains an estimate of the quantitative molecular density within the cell that is substantially more accurate than the unprocessed image. Individual optical sections were inspected and analysed using computer graphics software. The software for processing and analysis of images was on a Silicon Graphics workstation. The software is now available for a PC from CSP, Inc. (Billerica, MA). In cells that were stained for two different classes of molecules utilizing two different coloured fluorophores, we assessed the extent to which the two molecules were similarly distributed by combining the two images and coding information in each of the two image pairs in two different colours (typically red and green); when a pixel contained signal above threshold from both molecules it was white. The threshold level was set to exclude extranuclear background fluorescence in the case of visualization of 12CA5, or nucleoplasmic labelling in the case of visualization of RL1 and 1875. This background represented <30% of the specific signal in all cases and usually <5%.

Yeast molecular techniques

Methods used for yeast splicing extract preparation, extract fractionation, immunoprecipitation and RNA preparation were as previously described (Abovich et al., 1990). Western blots were carried out as described in Sambrook et al. (1989). Primary antibodies were used at dilutions indicated in the text, and proteins were detected with a streptavidin alkaline phosphatase-based system (Amersham).

Acknowledgements

We thank S.Baserga, F.Galissou, L.Gerace, P.Legrain, J.Steitz, I.Wilson and L.Zweibel for antibody reagents, and P.Kolodziej and R.Young for the epitope-tagged RNA polymerase II strain. We are grateful to K.Carter, J.Lawrence, W.Carrington and K.Fogarty for technical advice, for communication of unpublished results and for access to their new image restoration programs prior to publication. We thank members of the Rosbash lab for their comments on the work and the manuscript. Helpful comments on the manuscript were also made by B.Seraphin, P.Legrain, L.Davis, J.Lawrence and K.Carter. Secretarial assistance was provided by T.Tishman. This work was supported by grants from the NIH to M.R. and F.S.F., from the NSF Instrumentation Program to F.S.F., and from the Human Frontier Science Program to D.J.E.

References

- Abovich, N., Legrain, P. and Rosbash, M. (1990) *Mol. Cell. Biol.*, **10**, 6417–6425.
 Agard, D.A., Hiraoka, Y., Shaw, P. and Sedat, J.W. (1989) *Methods Cell Biol.*, **30**, 353–377.
 Bindereif, A. and Green, M.R. (1987) *EMBO J.*, **6**, 2415–2424.
 Brody, E. and Abelson, J. (1985) *Science*, **288**, 963–967.
 Carrington, W.A., Fogarty, K.E. and Fay, F.S. (1990) In Fosbitt, K. and Grinstein, S. (eds), *Non-invasive Techniques in Cell Biology*. Wiley-Liss, New York, pp. 53–72.
 Carter, K.C., Taneja, K.L. and Lawrence, J.B. (1991) *J. Cell Biol.*, **115**, 1191–1202.
 Carmo-Fonseca, M., Tollervey, D., Pepperkok, R., Barabino, S. Merdes, A.,

- Brunner, C., Zamore, P.D., Green, M.R., Hurt, E. and Lamond, A.I. (1991) *EMBO J.*, **10**, 195–206.
 Carmo-Fonseca, M., Pepperkok, R., Carvalho, M.T. and Lamond, A.I. (1992) *J. Cell Biol.*, **117**, 1–14.
 Chang, T.-H., Clark, M.W., Lustig, A.J., Cusick, M.E. and Abelson, J. (1988) *Mol. Cell. Biol.*, **8**, 2379–2393.
 Davis, L.I. and Fink, G.R. (1990) *Cell*, **61**, 965–968.
 Fakan, S. and Puvion, E. (1980) *Int. Rev. Cytol.*, **65**, 255–299.
 Fay, F.S., Carrington, W.A. and Fogarty, K.E. (1989) *J. Microscopy*, **153**, 133–149.
 Frendewey, D. and Keller, W. (1985) *Cell*, **42**, 355–367.
 Fu, X.-D. and Maniatis, T. (1990) *Nature*, **343**, 437–441.
 Gall, J.G. (1991) *Science*, **252**, 1499–1500.
 Grabowski, P.J. and Sharp, P.A. (1986) *Science*, **233**, 1294–1299.
 Grabowski, P.J., Seiler, S.R. and Sharp, P.A. (1985) *Cell*, **42**, 345–353.
 Green, M.R. (1991) *Annu. Rev. Cell Biol.*, **7**, 559–599.
 Guthrie, C. (1991) *Science*, **253**, 157–163.
 Hall, M.N., Craik, C. and Hiraoka, Y. (1990) *Proc. Natl. Acad. Sci. USA*, **87**, 6954–6958.
 Hirano, T., Kinoshita, N., Morikawa, K. and Yanagida, M. (1990) *Cell*, **60**, 319–328.
 Huang, S. and Spector, D.L. (1992) *Proc. Natl. Acad. Sci. USA*, **89**, 305–308.
 Hurt, E.C. (1988) *EMBO J.*, **7**, 4323–4334.
 Hurt, E.C., McDowell, A. and Schimmang, T. (1988) *Eur. J. Cell Biol.*, **46**, 554–563.
 Jackson, D.A. (1991) *BioEssays*, **13**, 1–10.
 Kolodziej, P.A., Woychik, N., Liao, S.-M. and Young, R.A. (1990) *Mol. Cell. Biol.*, **10**, 1915–1920.
 Konarska, M.M. and Sharp, P.A. (1987) *Cell*, **49**, 763–774.
 Lamm, G.M., Blencowe, B.J., Sproat, B.S., Iribarren, A.M., Ryder, U. and Lamond, A.I. (1991) *Nucleic Acids Res.*, **190**, 3193–3198.
 Lamond, A.I., Konarska, M.M., Grabowski, P.J. and Sharp, P.A. (1988) *Proc. Natl. Acad. Sci. USA*, **85**, 411–415.
 Legrain, P. and Choulika, A. (1990) *EMBO J.*, **9**, 2775–2781.
 Legrain, P. and Rosbash, M. (1989) *Cell*, **57**, 573–583.
 Legrain, P., Chapon, C. and Galissou, F. (1991) *Nucleic Acids Res.*, **19**, 2509–2510.
 Li, H. and Bingham, P.M. (1991) *Cell*, **67**, 335–342.
 Maul, G.G. (1977) *Int. Rev. Cytol.*, **6**, 75–186.
 Nehrbass, U., Kern, H., Mutvei, A., Horstmann, H., Marshallsay, B. and Hurt, E.C. (1990) *Cell*, **61**, 979–989.
 Pikielny, C.W., Rymond, B.C. and Rosbash, M. (1986) *Nature*, **324**, 341–345.
 Potashkin, J.A., Derby, R.J. and Spector, D.L. (1990) *Mol. Cell. Biol.*, **10**, 3524–3534.
 Rosbash, M. and Séraphin, B. (1991) *Trends Biochem. Sci.*, **16**, 187–190.
 Rosbash, M., Harris, P.K.W., Woolford, J.L., Jr and Teem, J.L. (1981) *Cell*, **24**, 679–686.
 Ruby, S.W. and Abelson, J. (1991) *Trends Genet.*, **7**, 79–85.
 Sambrook, J., Fritsch, E.F. and Maniatis, T. (1989) *Molecular Cloning: A Laboratory Manual*. Cold Spring Harbor Laboratory Press, Cold Spring Harbor, NY.
 Séraphin, B. and Rosbash, M. (1989) *Cell*, **59**, 349–358.
 Séraphin, B., Abovich, N. and Rosbash, M. (1991) *Nucleic Acids Res.*, **19**, 3857–3860.
 Siliciano, P.G., Brow, P.A., Roiha, H. and Guthrie, C. (1987) *Cell*, **50**, 585–592.
 Spector, D.L. (1990) *Proc. Natl. Acad. Sci. USA*, **87**, 147–151.
 Spector, D.L., Fu, X.-D. and Maniatis, T. (1991) *EMBO J.*, **10**, 3467–3481.
 Vijayraghavan, U., Company, M. and Abelson, J. (1989) *Genes Dev.*, **3**, 1206–1216.
 Wang, J., Cao, L.-G., Wang, Y.-L. and Pederson, T. (1991) *Proc. Natl. Acad. Sci. USA*, **88**, 7391–7395.
 Zamore, P.D. and Green, M.R. (1991) *EMBO J.*, **10**, 207–214.
 Zamore, P.D., Patton, J.G. and Green, M.R. (1992) *Nature*, **355**, 609–614.

Received on May 5, 1992; revised on June 19, 1992